NTIA Report TR-12-483

A Prototype Antenna for Total RF Field Measurement

J. Wayde Allen

NTIA

report series

U.S. DEPARTMENT OF COMMERCE • National Telecommunications and Information Administration

NTIA Report TR-12-483

A Prototype Antenna for Total RF Field Measurement

J. Wayde Allen

U.S. DEPARTMENT OF COMMERCE

October 2011

DISCLAIMER

CONTENTS

A PROTOTYPE ANTENNA FOR TOTAL RF FIELD MEASUREMENT

J. Wayde Allen[1]

The total radio frequency (RF) field strength is the sum of all signals incident at a given location. These signals can originate from many directions and have various polarizations. This complicates the measurement of the total RF field since commonly used antennas (dipoles, whips, etc.) respond to signals coming from a specific direction and with a specific polarization.

This paper describes a prototype antenna constructed from three crossed dipole elements. The output from these three dipole elements can be used to detect signals having arbitrary polarization, and arriving from any direction. This makes it possible to perform real-time measurement of the total RF field.

Key words: antenna; crossed dipole; electromagnetic; electro-space; environment; noise; polarization; radio; RF; spectrum survey; Table Mountain

1 INTRODUCTION

At any arbitrary location, the total radio frequency (RF) field strength is the sum of the radio signals arriving at that location. These signals can arrive from many different directions and have varying polarizations. Unfortunately, antennas commonly used for measuring these signals (vertical whips, dipoles, Yagi arrays, etc.) respond most strongly to signals having a specific polarization or arriving from a certain direction. Consequently radio surveys are generally limited to vertically or horizontally polarized signals. In some cases, diagonally mounted Yagi antennas are used so that the response to horizontal and vertical polarizations are roughly equal, but this only works for signals originating from the direction in which the Yagi is pointed. This leaves us with two options for measuring the total field strength:

- make repeat measurements using more than one antenna type and/or orientation, or
- create several measurement systems configured with different antennas.

The first option uses the least amount of receiver hardware, but is time consuming and makes the assumption that the field is relatively static so that measurements from different time series can be reasonably combined. The second option uses multiple receivers, which can be more expensive, but takes less time to perform and will work with time varying signals. In either case, an antenna combination needs to be chosen that minimizes the number of tests or receivers needed, and that makes combining these data straight forward. This paper describes an antenna array designed specifically for this purpose.

[1]The author is with the Institute for Telecommunication Sciences, National Telecommunications and Information Administration, U.S. Department of Commerce, Boulder, Colorado 80305.

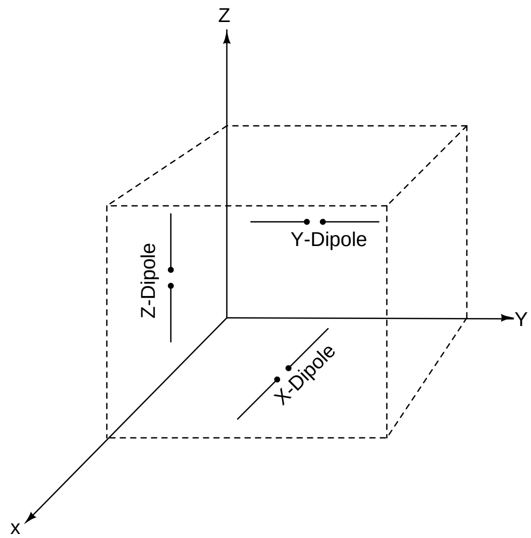

Figure 1: Dipole antennas relative to a 3D reference cube.

This antenna array consists of three orthogonal dipole antennas oriented as shown in Figure 1. In this configuration, each dipole element responds most strongly to linearly polarized signals that match the axis of the antenna element, and which are incident at right angles to the plane in which the antenna element resides. The output from each of the dipole elements in this array is proportional to the vector field components $\overline{E_x}$, $\overline{E_y}$, and $\overline{E_z}$. This concept has been used for the construction of various EM radiation monitors, but these are usually only coupled to square law power detectors and no phase information is preserved. Positioning the elements adjacent to each other and sampling the E-field components simultaneously preserves phase information.

A prototype crossed dipole array like this was constructed in the early 1980's at the National Bureau of Standards (now the National Institute for Standards and Technology or NIST)[1][2]. The NIST design used mechanical switching to alternately connect the dipole antennas to a single back-end spectrum analyzer. This allowed total field measurements in the presence of signals that didn't change during the time interval required to switch between the antenna elements. However, since readings were taken sequentially rather than simultaneously, the instantaneous total field could not be measured, and again phase information was lost.

The system described here uses a true three channel receiver capable of recording the E-field voltages induced in each of the dipoles in synchronous real-time. This makes it possible not only to gather information about the total RF field strength regardless of direction of arrival, but also to distinguish polarization, and possibly even direction of arrival.

2 DESIGN OF THE ANTENNA

The antenna consists of an array of three orthogonally arranged dipole elements, each with its own tuning filter and preamplifier feeding a separate channel on a digitizing oscilloscope. Figure 2 shows a basic block diagram of the circuit.

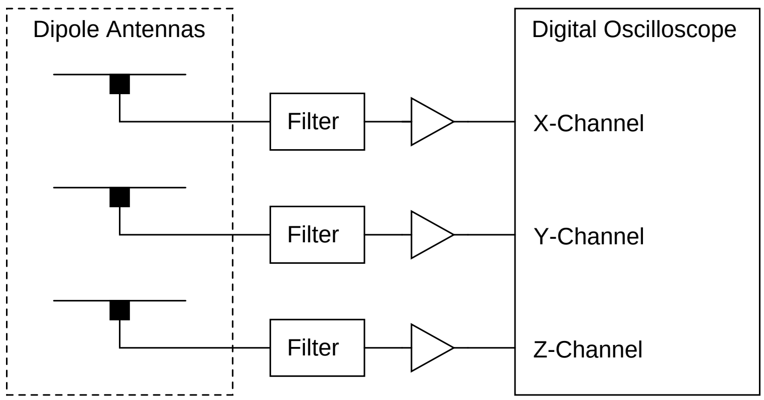

Figure 2: Block diagram of the antenna system.

This decision allows us to tune the array to a specific frequency range using the filters, and to capture time domain data of the signal as detected by the X, Y, and Z dipole elements.

We wanted to make the dipole elements tunable to test at different frequencies. A vendor was found that could provide telescoping antenna elements that could be adjusted from 17.78 to 71.12 centimeters (7 to 28 inches), giving a useable frequency range of approximately 100 to 401 MHz. Plastic mounting blocks were made to hold these elements in appropriate orientation to each other. Two of these blocks were made.

The first of these blocks was made with the mounting support hole drilled parallel to the Z-axis dipole. This configuration simplifies testing by eliminating the need for transforming our data between the antenna and laboratory coordinate systems, and consequently is the focus of this paper. The resulting structure is shown in Figure 3.

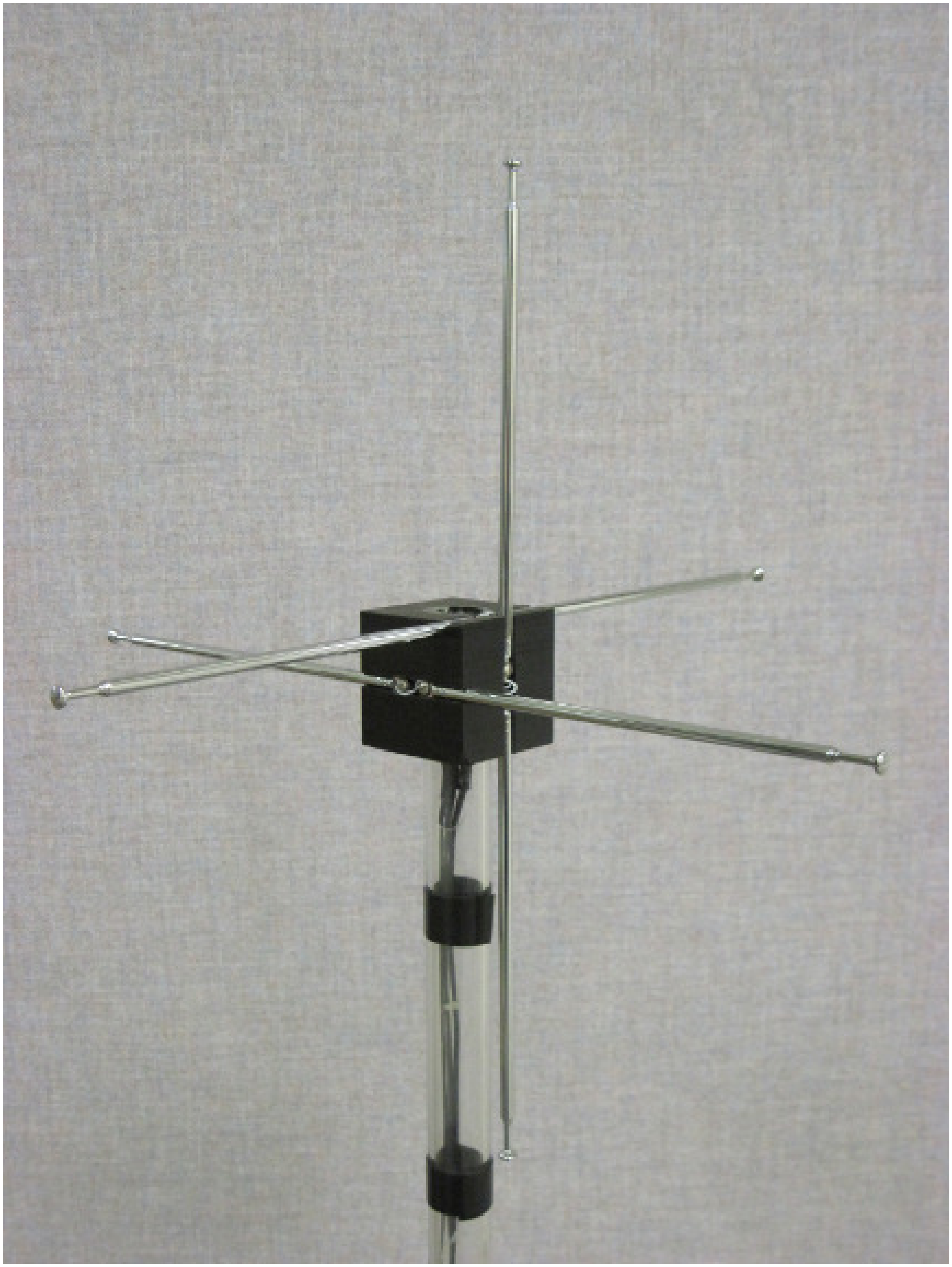

Figure 3: Picture of the crossed dipole array arranged with elements relative to the laboratory coordinate system.

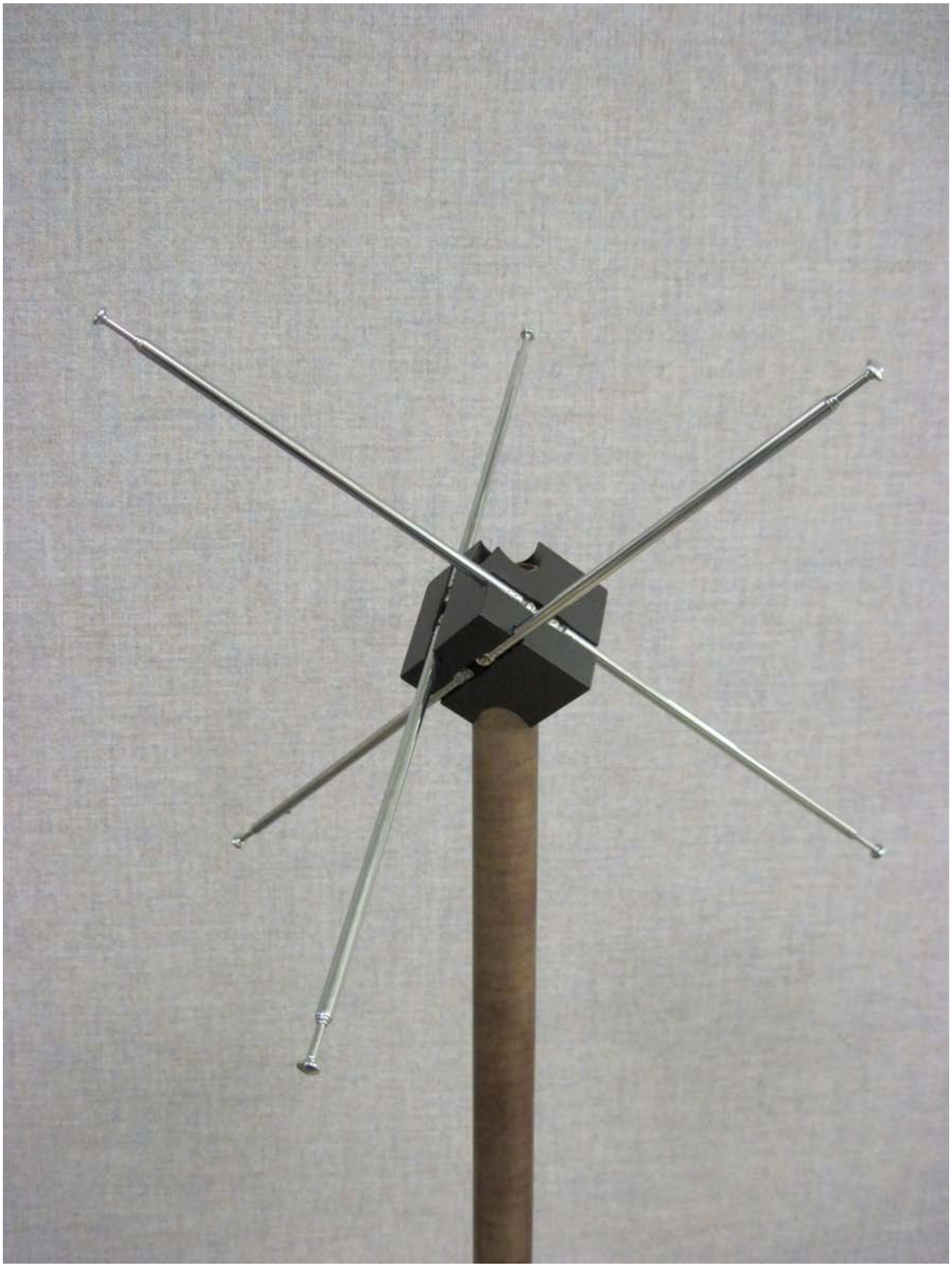

Figure 4: Picture of the diagonal mounting block.

In the second block, the mounting support rod runs along the diagonal of the block as shown in Figure 4. This diagonal mount design has the advantage of orienting each antenna element symmetrically around the support structure. A problem with this configuration is that it tips the XY-plane described by the X and Y antenna elements so that it no longer is parallel to the surface of the earth. For terrestrial systems, horizontal and vertical polarization is generally defined relative to the "laboratory frame of reference" where the XY-plane is parallel to the surface of the earth. This means that using the antenna constructed with the diagonal mounting block requires a coordinate system transformation to get E'_x, E'_y, and E'_z into the laboratory frame of reference E_x, E_y, and E_z. Testing of the diagonal mounting block has not been completed and will not be discussed in this paper.

Broadband balun transformers are used to connect the dipole elements to the coaxial feed that runs down through a piece of 1 inch plastic tubing that provides the mounting support for the antenna.

3 PROOF OF CONCEPT TESTING

We ran three basic tests to see if this 3-axis antenna design concept worked as expected:

1. Test the response of the 3-axis antenna to various polarized signals incident from different directions.
2. Verify that the antenna response would show the total incident power proportional to $|E_x|^2 + |E_y|^2 + |E_z|^2$ regardless of the polarization or angle of incidence.
3. Measure the antenna transmission pattern with each of the elements driven with in-phase signals and compare this to a computer simulation using an NEC model.

The setup for the first two tests used a Yagi antenna driven by a signal generator set to 402.5 MHz and a power of 10 dBm. This frequency is slightly higher than the predicted resonance of the antenna, but not appreciably so. The decision to use this frequency was driven by the availability of an existing three channel filter/amplifier box. The Yagi antenna was mounted on a tripod in the NIST anechoic chamber with the 3-axis receive antenna mounted on the antenna rotator. This allowed the Yagi to present a fixed level signal with a polarization relative to its orientation (horizontal, 45 degree slant, or vertical). The output of the 3-axis antenna was connected to the filter/amplifier box to provide selectivity and gain and the resulting channels for $\overline{E_x}$, $\overline{E_y}$, and $\overline{E_z}$ were fed into a digitizing oscilloscope. Figure 5 shows a block diagram, and Figure 6 shows a photograph of the actual test setup. Plots of the measured voltages E_x, E_y, and E_z data can be seen in Figures 7–15.

As can be seen, the relative amplitudes of the traces do seem to vary as expected with respect to the polarization angle and angle of incidence. Also, since the transmit power was held constant during the measurements these data can be used to verify whether the total received power is proportional to $|E_x|^2 + |E_y|^2 + |E_z|^2$. This satisfies the data acquisition for the first two verification tests.

The third and last test is to see if the real-life antenna array performs as predicted by the NEC model. This requires reconfiguring the antennas as shown in Figure 16.

For this test, the 3-axis antenna is the transmit antenna, and is fed by a signal generator through a power splitter providing three in-phase signals to each of the three dipoles in the array. The Yagi array was used as a fixed, horizontally polarized, receive antenna connected to a power meter. The 3-axis antenna was then oriented at five tilt angles (0 degrees, 22.5 degrees, 45 degrees, 67.5 degrees, and 90 degrees) as shown in Figure 17. In this case 0 degrees corresponds to the antenna standing vertically upright and 90 degrees corresponds to the antenna tipped forward to a fully horizontal position. In all but the 90 degree position the antenna was then rotated in 5 degree increments around its axis and the received power seen by the Yagi antenna was recorded at each of these intervals. Fewer points were taken at the 90 degree position since the Yagi was aimed straight down onto the 3-axis antenna at this point.

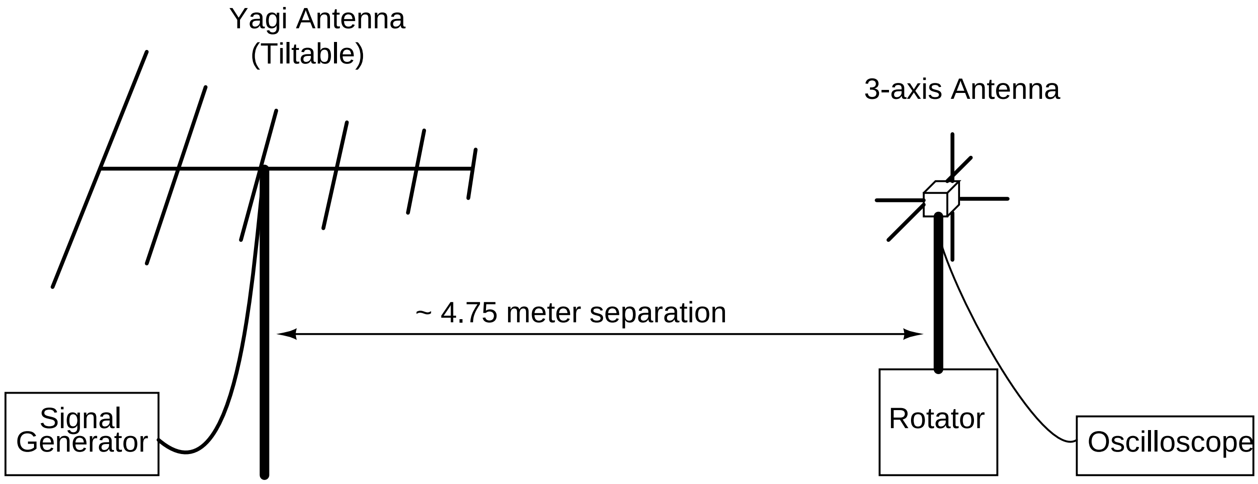

Figure 5: Block diagram of the test setup.

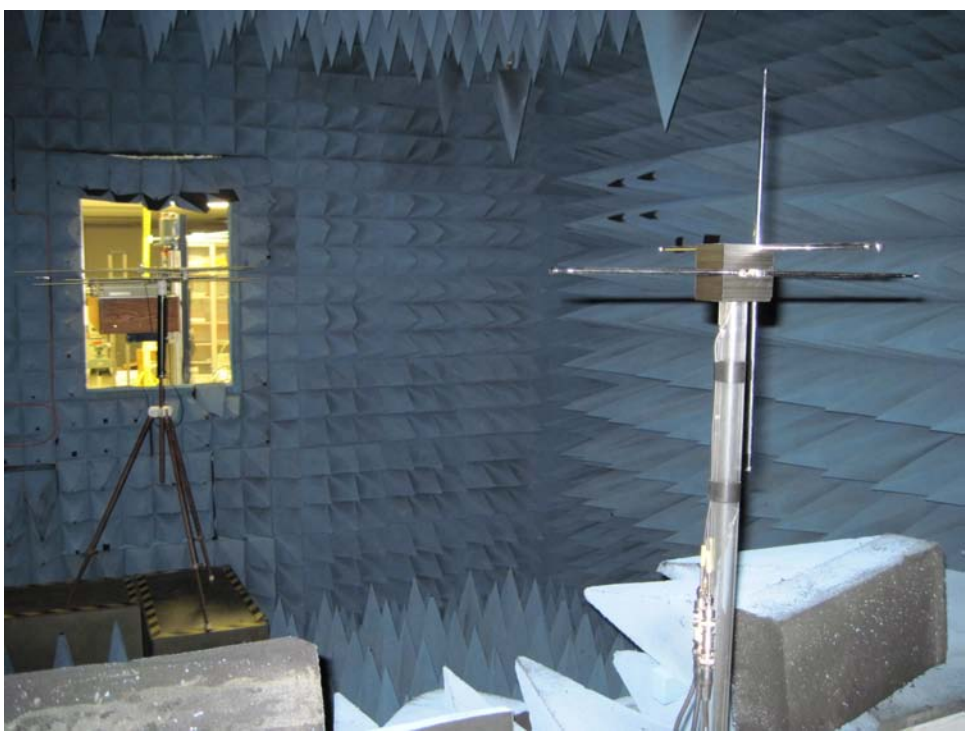

Figure 6: Photograph of the test setup.

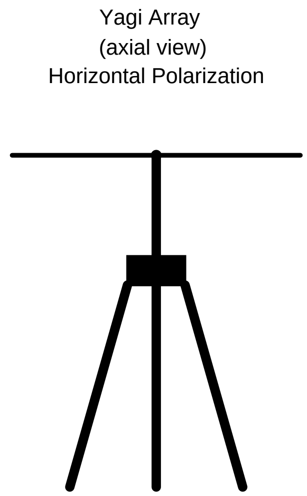

(a) Yagi Antenna Orientation

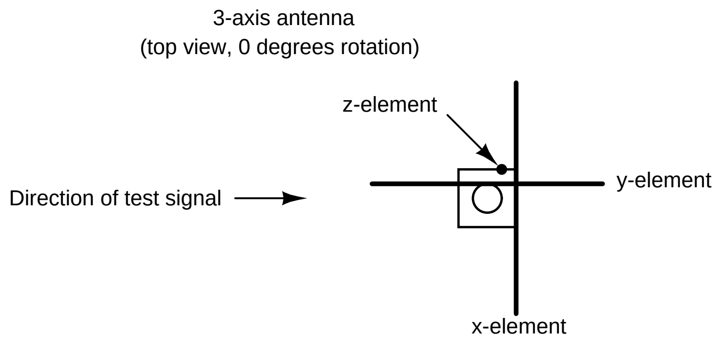

(b) 3-axis Antenna Orientation

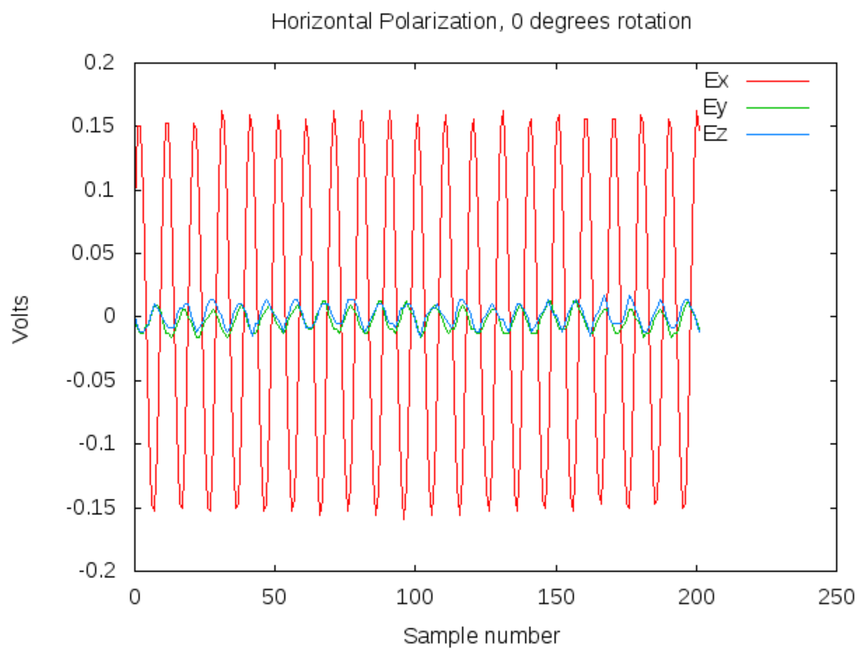

(c) Plot of oscilloscope trace (5 nSec trace, 202 samples).

Figure 7: Measurement with horizontal Yagi antenna, and 3-axis antenna not rotated. Graphic (a) shows the Yagi antenna orientation. Graphic (b) shows the 3-axis antenna rotation, and (c) shows the resulting oscilloscope trace.

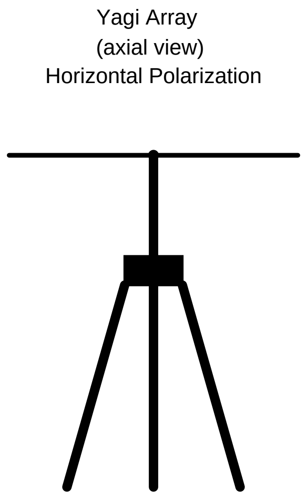

(a) Yagi Antenna Orientation

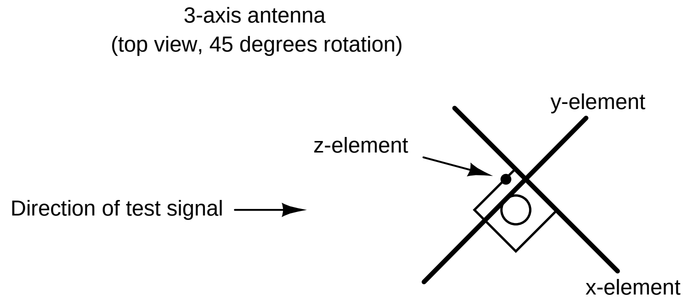

(b) 3-axis Antenna Orientation

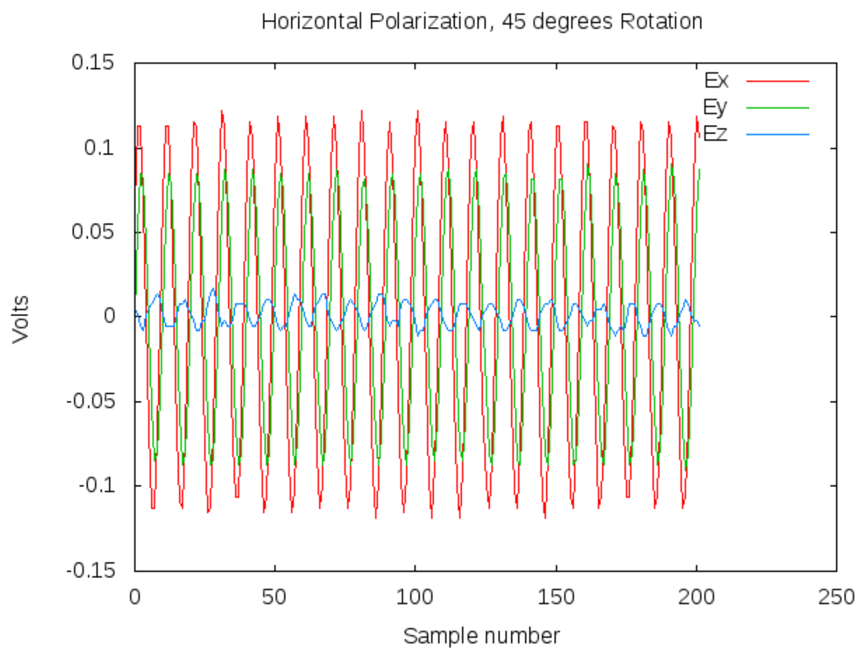

(c) Plot of Oscilloscope trace (5 nSec trace, 202 samples).

Figure 8: Measurement with horizontal yagi antenna, and 3-axis antenna rotated 45 degrees. Graphic (a) shows the Yagi antenna orientation. Graphic (b) shows the 3-axis antenna rotation, and (c) shows the resulting oscilloscope trace.

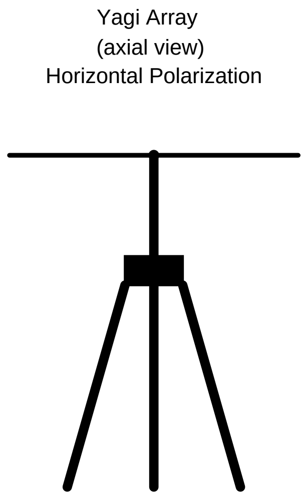

(a) Yagi Antenna Orientation

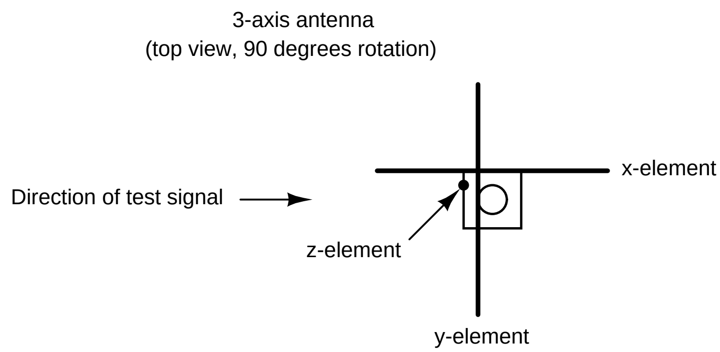

(b) 3-axis Antenna Orientation

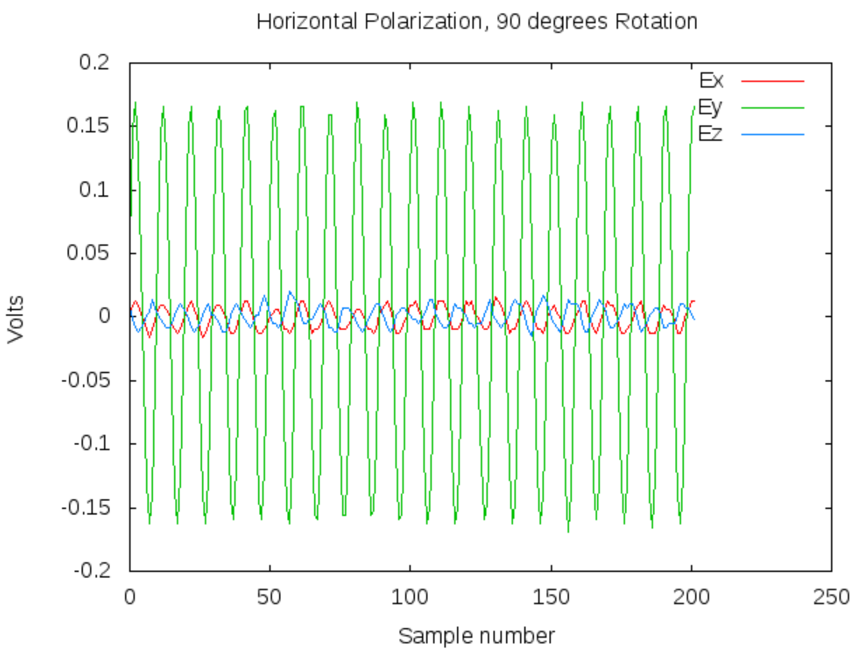

(c) Plot of Oscilloscope trace (5 nSec trace, 202 samples).

Figure 9: Measurement with horizontal yagi antenna, and 3-axis antenna rotated 90 degrees. Graphic (a) shows the Yagi antenna orientation. Graphic (b) shows the 3-axis antenna rotation, and (c) shows the resulting oscilloscope trace.

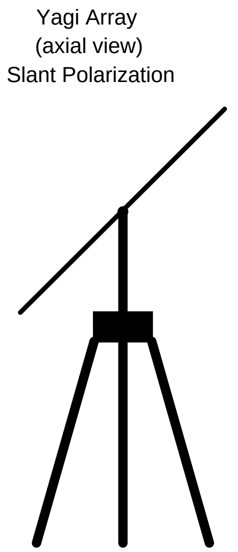

(a) Yagi Antenna Orientation

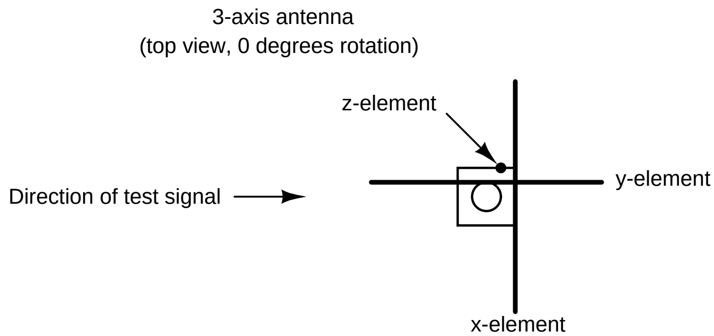

(b) 3-axis Antenna Orientation

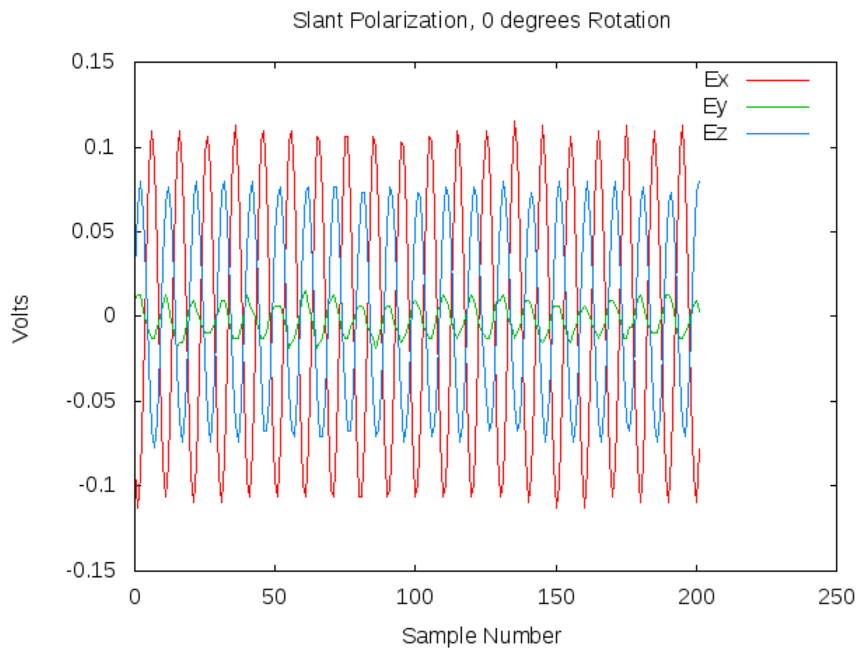

(c) Plot of Oscilloscope trace (5 nSec trace, 202 samples).

Figure 10: Measurement with slant polarized yagi, and 3-axis antenna not rotated. Graphic (a) shows the Yagi antenna orientation. Graphic (b) shows the 3-axis antenna rotation, and (c) shows the resulting oscilloscope trace.

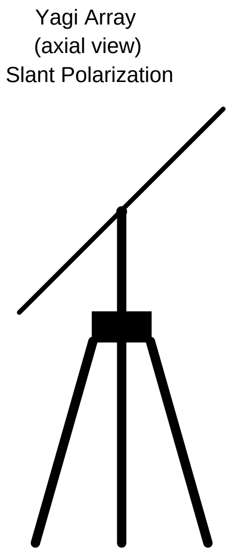

(a) Yagi Antenna Orientation

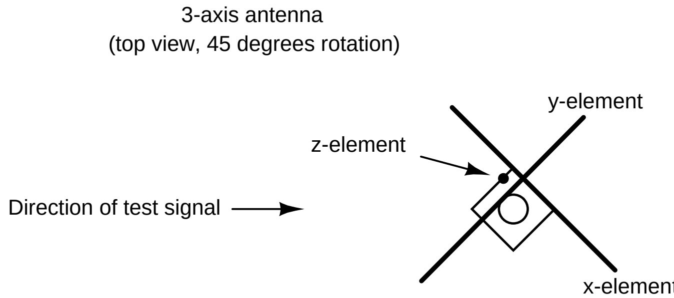

(b) 3-axis Antenna Orientation

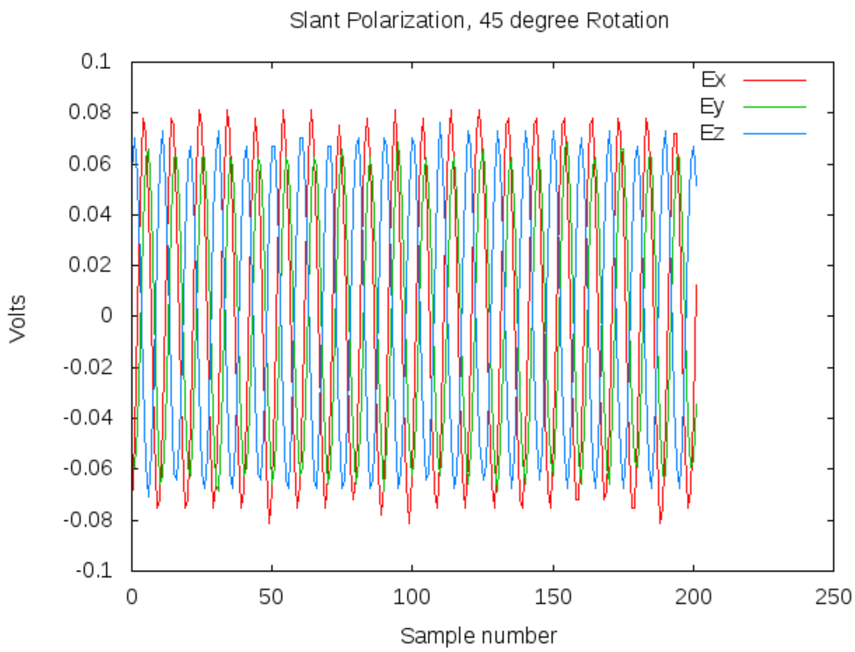

(c) Plot of Oscilloscope trace (5 nSec trace, 202 samples).

Figure 11: Measurement with slant polarized yagi, and 3-axis antenna rotated 45 degrees. Graphic (a) shows the Yagi antenna orientation. Graphic (b) shows the 3-axis antenna rotation, and (c) shows the resulting oscilloscope trace.

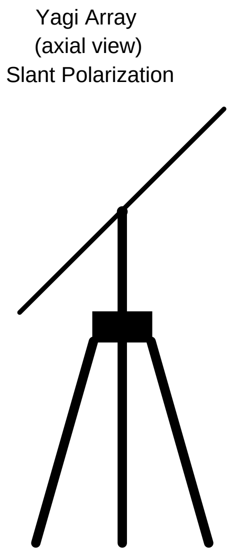

(a) Yagi Antenna Orientation

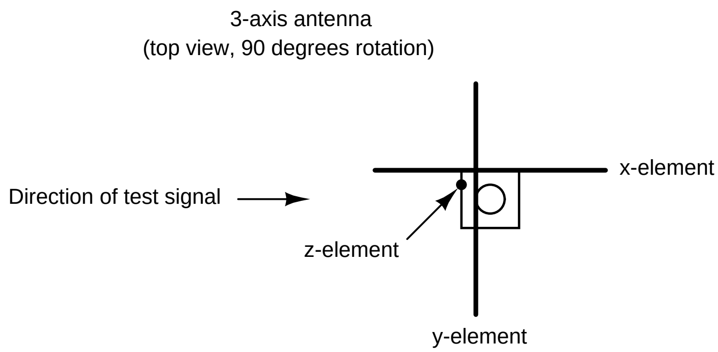

(b) 3-axis Antenna Orientation

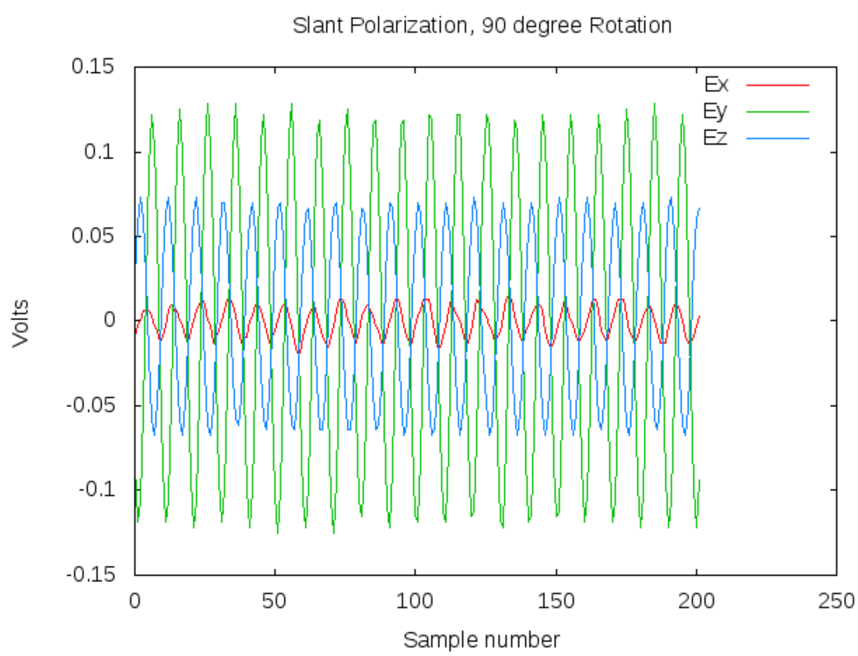

(c) Plot of Oscilloscope trace (5 nSec trace, 202 samples).

Figure 12: Measurement with slant polarized yagi, and 3-axis antenna rotated 90 degrees. Graphic (a) shows the Yagi antenna orientation. Graphic (b) shows the 3-axis antenna rotation, and (c) shows the resulting oscilloscope trace.

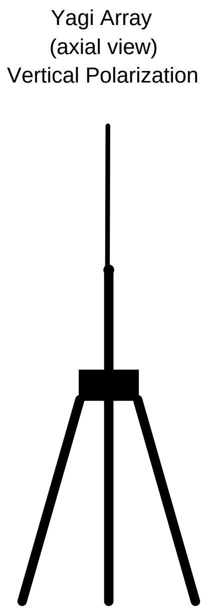

(a) Yagi Antenna Orientation

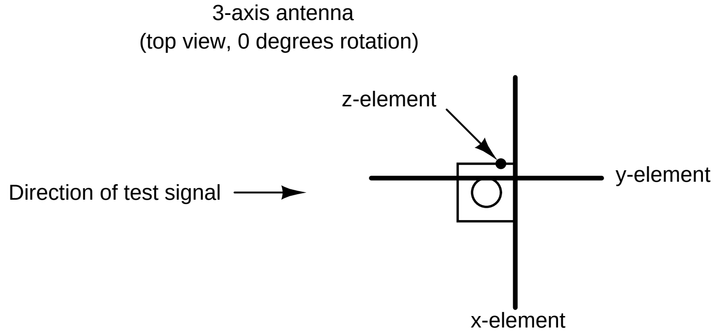

(b) 3-axis Antenna Orientation

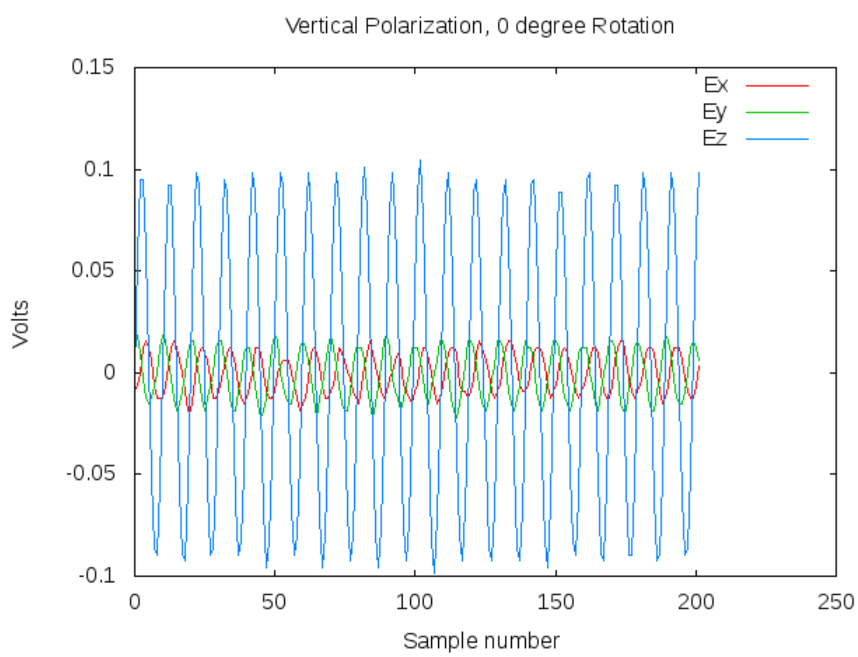

(c) Plot of Oscilloscope trace (5 nSec trace, 202 samples).

Figure 13: Measurement with vertically polarized yagi, and 3-axis antenna not rotated. Graphic (a) shows the Yagi antenna orientation. Graphic (b) shows the 3-axis antenna rotation, and (c) shows the resulting oscilloscope trace.

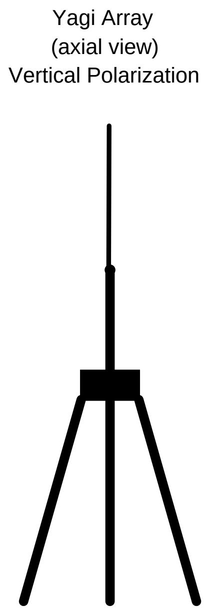

(a) Yagi Antenna Orientation

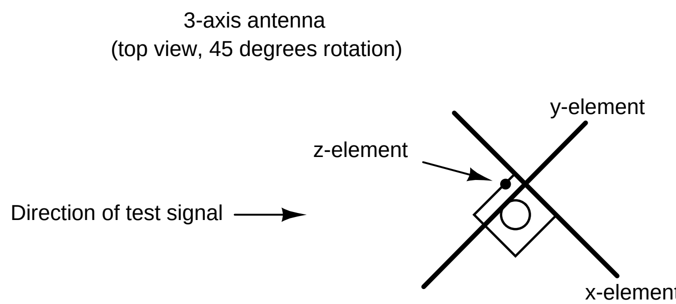

(b) 3-axis Antenna Orientation

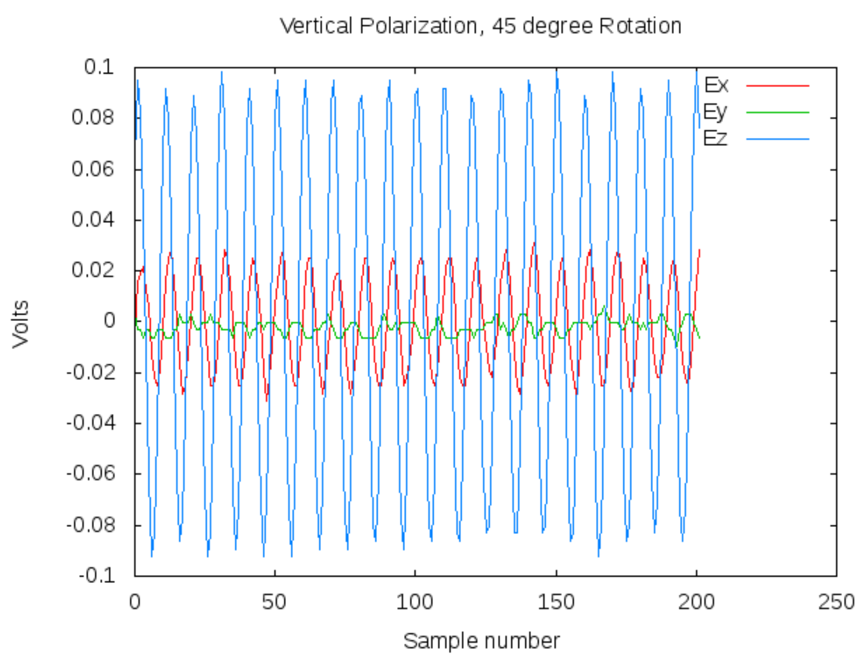

(c) Plot of Oscilloscope trace (5 nSec trace, 202 samples).

Figure 14: Measurement with vertically polarized yagi, and 3-axis antenna rotated 45 degrees. Graphic (a) shows the Yagi antenna orientation. Graphic (b) shows the 3-axis antenna rotation, and (c) shows the resulting oscilloscope trace.

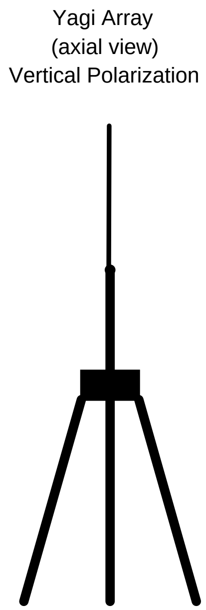

(a) Yagi Antenna Orientation

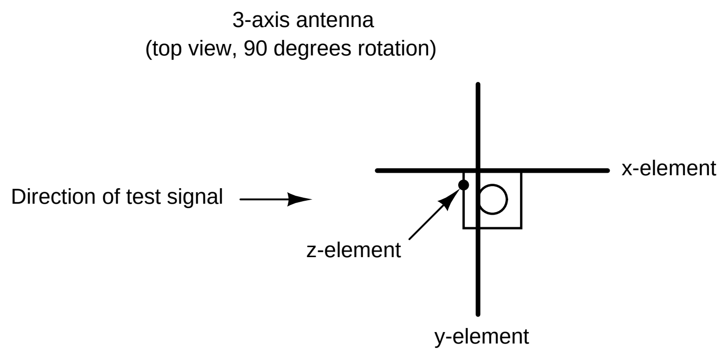

(b) 3-axis Antenna Orientation

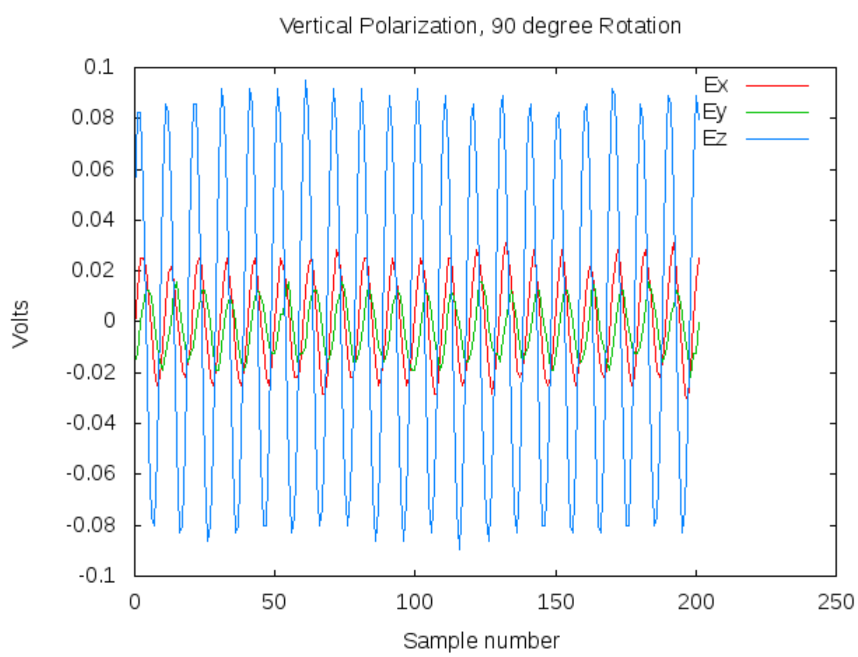

(c) Plot of Oscilloscope trace (5 nSec trace, 202 samples).

Figure 15: Measurement with vertically polarized yagi, and 3-axis antenna rotated 90 degrees. Graphic (a) shows the Yagi antenna orientation. Graphic (b) shows the 3-axis antenna rotation, and (c) shows the resulting oscilloscope trace.

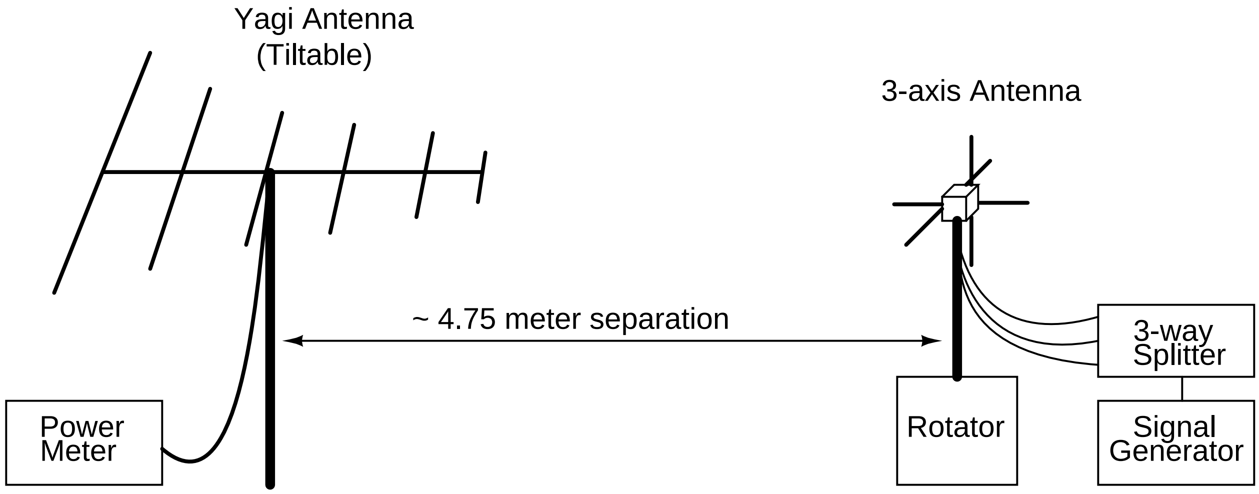

Figure 16: Antenna configuration for transmission pattern test.

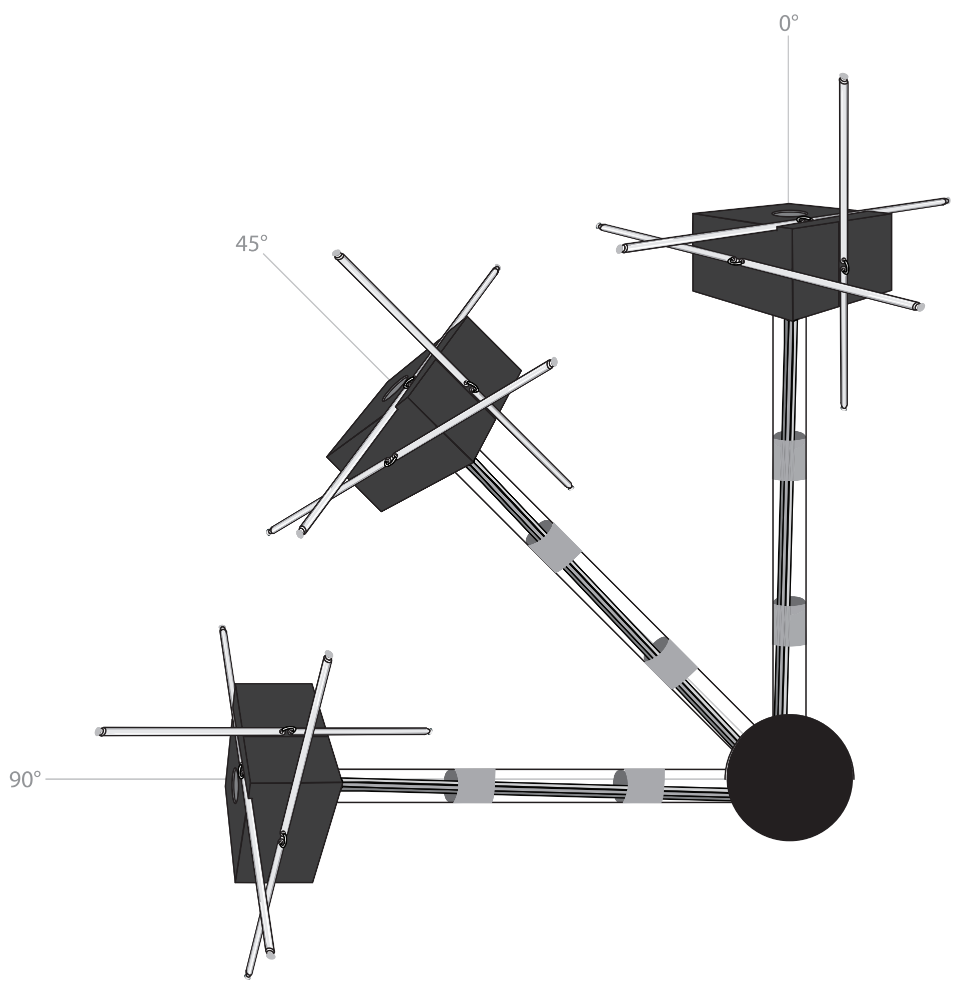

Figure 17: Tilt angles for the 3-axis antenna pattern measurement.

For comparison, a computer simulation using the Numerical Electrical Code (NEC) Method of Moments was set up as follows:

```
CM NEC Input for 3-axis Antenna
CM
CM Author: J.W. Allen
CM Date: 2010-08-13
CM
CM Element Diameter 0.00508 meters (0.2 inches)
CM Dipole is center fed with 17.78 cm (7 inches) to each side
CM Single frequency excitation at 421 MHz on the center (5th segment)
CM I've added 0.3175 cm (1/8 inch) to each side.
CM This creates a 0.635 cm (1/4 inch) feed gap.
CE
GW  1    9   -0.1809   -0.0100    0.0000    0.1809   -0.0100    0.0000   0.00508
GW  2    9    0.0100   -0.1809    0.0100    0.0100    0.1809    0.0100   0.00508
GW  3    9   -0.0100    0.0100   -0.1809   -0.0100    0.0100    0.1809   0.00508
GE
EX  0    1         5
EX  0    2         5
EX  0    3         5
RP  0   36   36 1301        0.        0.       10.       10.
PT  2    5         5         5
XQ
EN
```

Plots of both the measured and simulated antenna pattern can be seen in Figure 18. It is particularly interesting to note the deep null in the pattern that occurs along the diagonal of the coordinate system. This null appears to coincide with the diagonal of the plastic mounting block shown in Figure 4, which may be a reason to prefer the diagonal mount. This could minimize the effect of the support structure on the antenna performance. However, in this paper we report only tests of the structure designed to position the antenna elements parallel to the laboratory coordinate system.

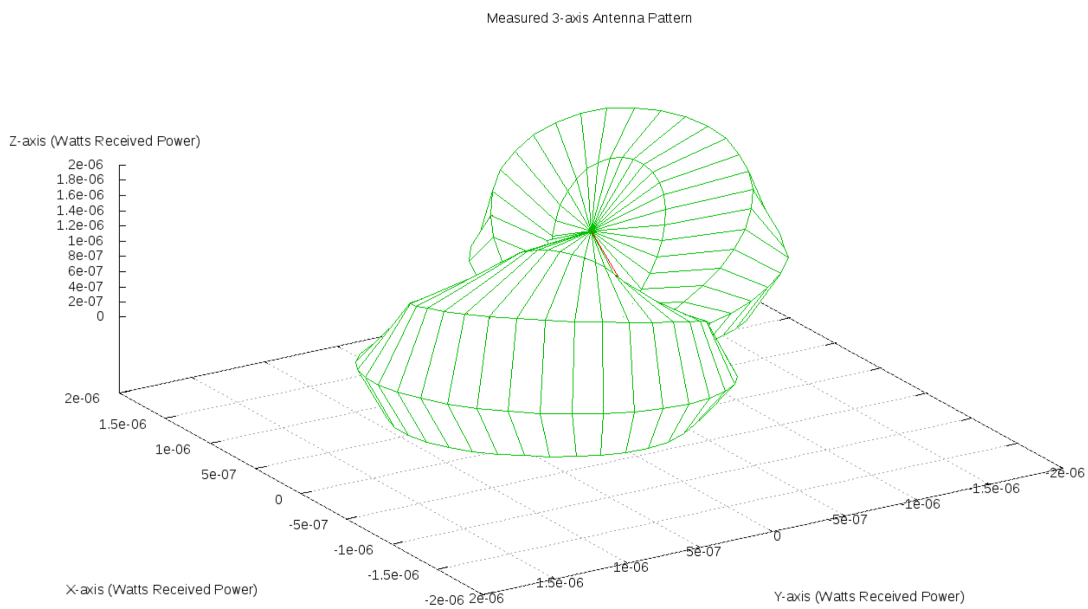

(a) Measured Antenna Pattern

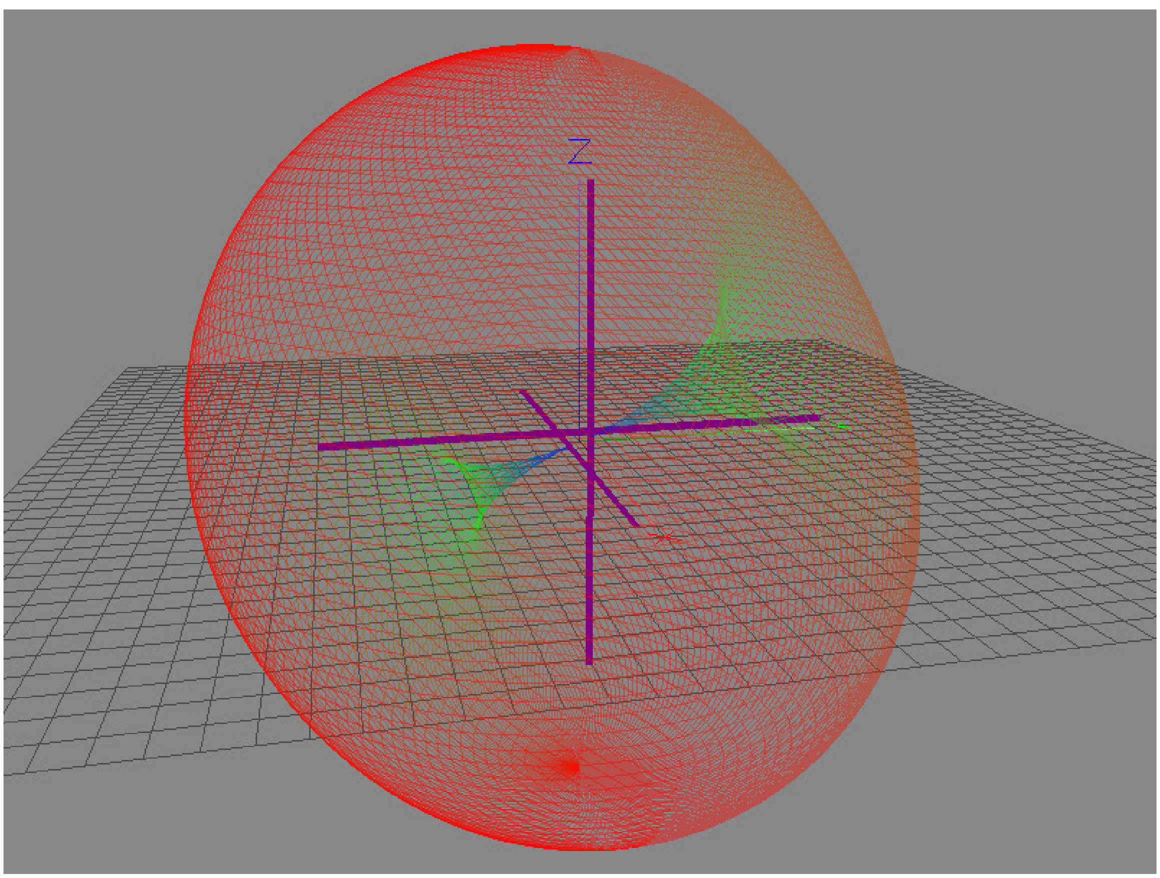

(b) Simulated Antenna Pattern

Figure 18: Comparison of the measured and simulated transmission pattern of the antenna with all elements fed in phase at the same frequency. Plot (a) shows the measured pattern, and plot (b) is the simulated pattern.

4 DATA ANALYSIS

4.1 Detecting polarization

Returning to the data plotted in Figures 7–15, we would like to find a way to clearly determine the polarization character of the incident signal. One way to do this is simply to plot the voltages E_x, E_y, and E_z in three dimensions so that we can see the shape described. For a horizontally polarized wave aligned with the X-axis antenna element, such a plot should describe a line with voltage excursions along the x-axis in the plot. Figure 7 shows the oscilloscope traces for this condition, so re-plotting these data in three dimensions results in the graph seen in Figure 19.

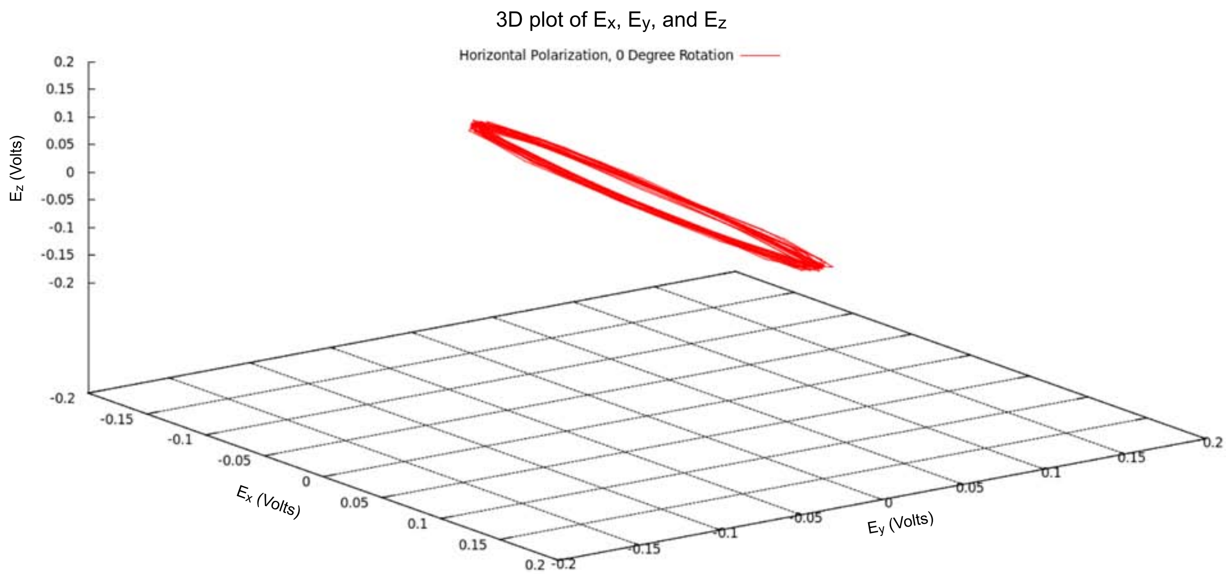

Figure 19: Plot of E_x, E_y, and E_z for the horizontally polarized signal at 0 degrees rotation (aligned with x-axis).

This plot shows these data are close to the predicted horizontal line along the X-axis. The deviation from the expected line is most likely due to measurement system noise and coupling between the other orthogonal antenna elements and chamber reflections.

Plotting the horizontally-polarized data for each of the measured rotation angles (0 degrees, 45 degrees, and 90 degrees) produces the plot shown in Figure 20a. Here we can see how the antenna array responds to the same horizontally polarized signal incident from these three different angles. Ideally, all three traces should be straight lines, but because the wave is partially incident on both the X and Y antenna elements, coupling between the two elements distorts the straight line character of the plot.

Finally plotting all of the measured polarizations and rotation angles results in Figure 20b. Here we can see that the general trend to render linearly polarized signals as narrow ellipses relative to the polarization angle and angle of incidence is as expected. Ideally, each of these traces would scribe a line; however, imperfections in the antenna, coupling between elements, and system noise cause some distortion in the line traces. Whether some of these effects could be accounted for through antenna calibration is an area to be explored.

4.2 Total Power Measurement

The voltages measured from each of the elements on the 3-axis antenna are proportional to $\overline{E_x}$, $\overline{E_y}$, and $\overline{E_z}$, and since the time average power is proportional to the square of the E-field magnitude it should be possible to obtain the total power incident on the antenna as:

$$P_{total} = C_x|E_x|^2 + C_y|E_y|^2 + C_z|E_z|^2 \tag{1}$$

with C_x, C_y, and C_z being a calibration constants for each of the antenna elements.

We tabulated the averages of the square of the measured element voltages to obtain the results shown in Table 1.

Table 1: Average of the Squared Voltages for Each Antenna Element

Polarization	Rotation (degrees)	$\|E_x\|^2$	$\|E_y\|^2$	$\|E_z\|^2$
Horizontal	0	0.012838	0.000071	0.000067
Horizontal	45	0.006967	0.003866	0.000046
Horizontal	90	0.000073	0.013891	0.000059
Slant	0	0.006124	0.000079	0.002908
Slant	45	0.003064	0.002168	0.002466
Slant	90	0.000074	0.007611	0.002462
Vertical	0	0.000095	0.000153	0.004661
Vertical	45	0.000343	0.000012	0.004238
Vertical	90	0.000329	0.000116	0.003892

If we knew the calibration constants C_x, C_y, and C_z, these could be converted to powers using the expressions:

$$P_x = C_x|E_x|^2, \tag{2}$$

$$P_y = C_y|E_y|^2, and \tag{3}$$

$$P_z = C_z|E_z|^2. \tag{4}$$

Since the original design of the test was for relative rather than absolute powers, we can simply let C_x, C_Y, and $C_z = 1$.

Ideally, only one of the antenna elements should respond under the following conditions:

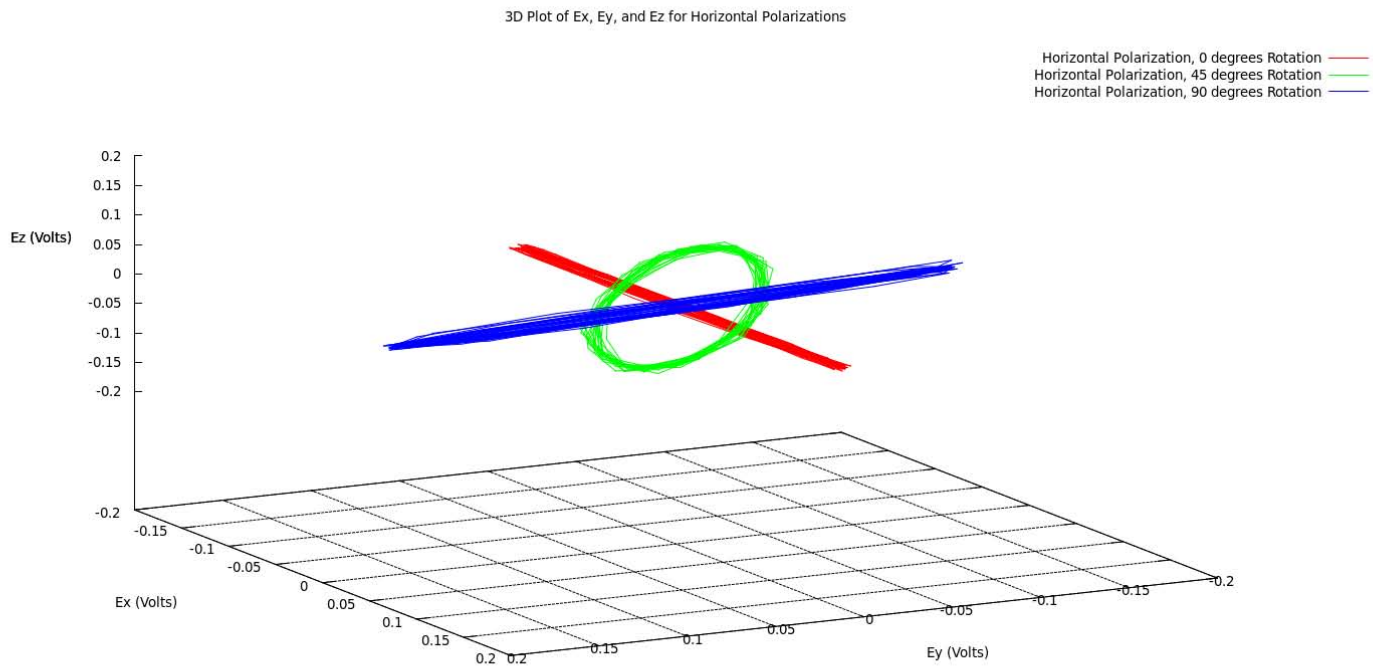

(a) Plot of the X, Y, and Z antenna element voltages for 0 degrees, 45 degrees, and 90 degrees rotation

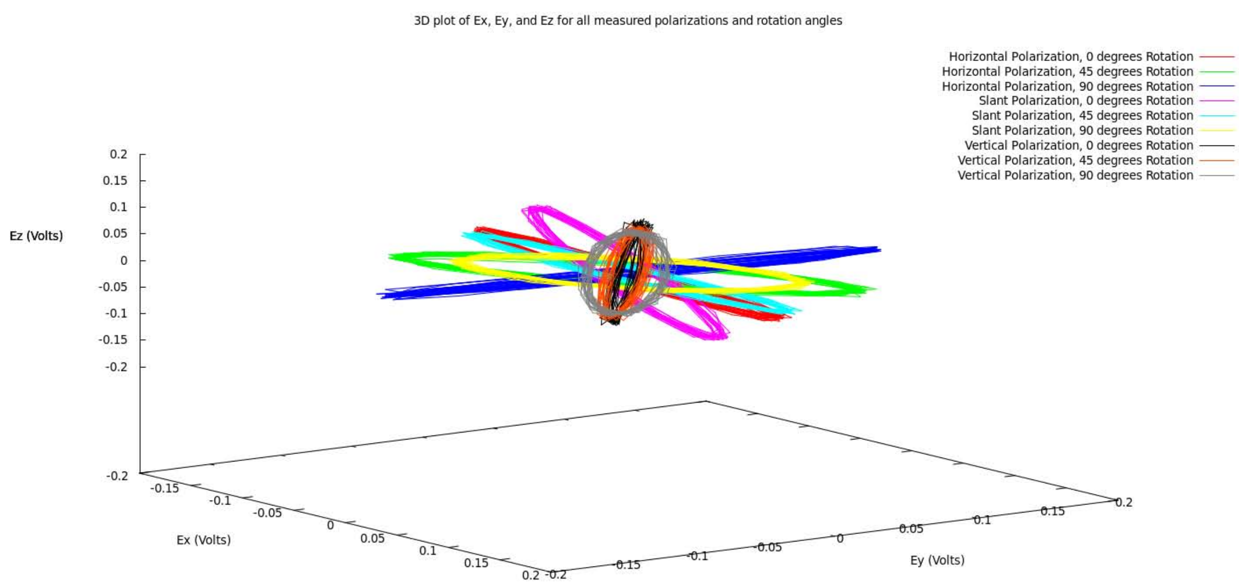

(b) Plot of Ex, Ey, and Ez for all measured polarizations and rotation angles

Figure 20: Plots of multiple polarization angles. Plot (a) shows the X, Y, and Z antenna element voltages for 0 degrees, 45 degrees, and 90 degrees rotation. Plot (b) shows Ex, Ey, and Ez for all measured polarizations and rotation angles.

1. Horizontal, 0 degrees Rotation—only E_x should receive power
2. Horizontal, 90 degrees Rotation—only E_y should receive power, and
3. Vertical, any rotation—only E_z should receive power

Unfortunately after looking at these data in Table 1, it became clear that the response of the Z-element dipole is less than that of the other two. Since we are still only interested in seeing whether the antenna system will give a constant power reading in any orientation, we can normalize these data so that each of these special case conditions results in a maximum reading of one. Taking the value for $|E_x|^2$ from the first row of Table 1 and substituting into (2) we obtain a value for C_x that normalizes our maximum power level for X-axis antenna element with the condition (horizontal, 0 degrees rotation) described above. This results in:

$$1 = C_x(0.012838), \tag{5}$$

or

$$C_x = 1/0.012838 \approx 77.893 \tag{6}$$

The E_y and E_z terms should ideally be zero, and as can be seen from Table 1 are small for this condition; we simply ignore them.

A similar computation performed for the Y-antenna element (horizontal, 90 degrees rotation) gives:

$$C_y = 1/0.013891 \ = 71.989. \tag{7}$$

For C_z all of the vertical polarized signal orientations work, so:

$$C_{z1} = 1/0.004661 \approx 214.565 \tag{8}$$

$$C_{z2} = 1/0.004238 \approx 235.971 \tag{9}$$

$$C_{z3} = 1/0.003892 \approx 256.917. \tag{10}$$

Taking the average of (8)–(10) gives us a useable value

$$C_z \approx 235.817 \tag{11}$$

Using these normalization coefficients to compute the average normalized powers gives the results in Table 2.

Table 2: Normalized Powers

Polarization	Rotation (degrees)	Normalized Power
Horizontal	0	1.021
Horizontal	45	0.832
Horizontal	90	1.020
Slant	0	1.168
Slant	45	0.976
Slant	90	1.134
Vertical	0	1.117
Vertical	45	1.027
Vertical	90	0.952
Maximum		1.168
Minimum		0.832
Difference		0.337
Average		1.027
Standard Deviation		0.104

From this, it appears that there is a Type B uncertainty [3] most likely due to calibration errors and cross coupling between the antenna elements that gives a reading too high by roughly 0.027, and a Type A random uncertainty [3] of roughly 0.104. Nevertheless, it seems that this antenna in this rather uncalibrated state can measure the total power regardless of polarization or angle of incidence to within roughly:

$$U_p = \sqrt{(0.027)^2 + (0.104)^2} \approx 0.107, \tag{12}$$

or with an uncertainty on the order of 10.7 percent. In decibels, this would be approximately ± 0.9 dB.

5 CONCLUSION

All the tests performed so far seem to indicate that the crossed-dipole, 3-axis antenna concept is viable. In fact, the idea is really not much different than using a single dipole receive antenna, and positioning it in a number of different orientations to sample RF energy coming from different directions, or even tilting it to change the polarization angle. What is unique about this configuration is that it allows data to be taken from each of the three dipoles simultaneously. This not only speeds up data acquisition, it also makes it possible to process the data stream to extract information about polarization and to compute the total RF field incident on the antenna. There are a number of avenues to explore to expand on this work.

Developing a good way to characterize or calibrate the array is one possible avenue. Another would be to change the diameter of the dipole elements, or use resistively loaded dipoles to extend the bandwidth of the antennas. The design used here is relatively narrow-banded, but using resistively loaded dipoles as was done by Kanda and Ries at NBS would be expected to expand the useable frequency range. Kanda and Ries reported that their original design had a relatively flat frequency response from 200 MHz to over 3 GHz [2].

The area that is particularly ripe for exploration would be how best to process data obtained using the array. We have already started exploring the use of software-defined radio systems to replace the digital oscilloscope used for these tests. This should help make the development of more complex, pseudo-real time data analysis possible.

Finally, as was shown with the NEC simulation and the transmit test, the interaction between the waves can create interesting nulls in the radiated pattern which may be useful to exploit. The test done here fed the antenna with in-phase signals. Changing the relative phases applied to each of the elements may make it possible to create controllable radiation patterns that could be used to steer or blank out the transmitted signal in particular regions.

6 REFERENCES

[1] M. Kanda and F. X. Ries, “A Broad-Band Isotropic Real-Time Electric-Field Sensor (BIRES) Using Resistively Loaded Dipoles,” *IEEE Transactions on Electromagnetic Compatibility*, vol. EMC-23, no. 3, August 1981.

[2] M. Kanda and F. X. Ries, “Dipole-Based EM Probe Grabs Complex Fields,” *Microwaves*, January 1981.

[3] B. N. Taylor and C. E. Kuyatt, “Guidelines for Evaluating and Expressing the Uncertainty of NIST Measurement Results,” National Institute of Standards and Technology, Tech. Rep. NIST Technical Note 1297, 1994.

Form NTIA-29 U.S. Department of Commerce
(6/04) National Telecommunications and Information Administration

BIBLIOGRAPHIC DATA SHEET

<table>
<tr><td>1. Publication Number
TR-12-483</td><td>2. Government Accession Number</td><td>3. Recipient's Accession Number</td></tr>
<tr><td colspan="2" rowspan="2">4. Title and Subtitle
A Prototype Antenna for Total RF Field Measurement</td><td>5. Publication Date</td></tr>
<tr><td>6. Performing Organization Code
NTIA/ITS</td></tr>
<tr><td colspan="2">7. Author(s)
J. Wayde Allen</td><td>9. Project/Task/Work Unit No.
3155011-300</td></tr>
<tr><td colspan="2">8. Performing Organization Name and Address
NTIA/ITS.M
U.S. Department of Commerce
325 Broadway
Boulder, CO 80305</td><td>10. Contract/Grant Number</td></tr>
<tr><td colspan="2">11. Sponsoring Organization Name and Address</td><td>12. Type of Report and Period Covered</td></tr>
<tr><td colspan="3">14. Supplementary Notes</td></tr>
<tr><td colspan="3">15. ABSTRACT (A 200-word or less factual summary of most significant information. If document includes a significant bibliography or literature survey, mention it here.)
The total radio frequency (RF) field strength is the sum of all signals incident at a given location. These signals can originate from many directions and have various polarizations. This complicates the measurement of the total RF field since commonly used antennas (dipoles, whips, etc.) respond to signals coming from a specific direction and with a specific polarization.
This paper describes a prototype antenna constructed from three crossed dipole elements. The output from these three dipole elements can be used to detect signals having arbitrary polarization, and arriving from any direction. This makes it possible to perform real-time measurement of the total RF field.</td></tr>
<tr><td colspan="3">16. Key Words (Alphabetical order, separated by semicolons)
antenna; crossed dipole; electromagnetic; electro-space; environment; noise; polarization; radio; RF; spectrum survey; Table Mountain</td></tr>
<tr><td rowspan="2">17. Availability Statement
[X] Unlimited
[ ] For Official Distribution</td><td>18. Security Class (This report)</td><td>20. Number of Pages
27</td></tr>
<tr><td>19. Security Class (This page)</td><td>21. Price</td></tr>
</table>